Laser and Particle Beams

cambridge.org/lpb

Forevacuum plasma source of continuous electron beam

Aleksandr Klimov[1], Ilya Bakeev[1], Efim Oks[1,2] and Aleksey Zenin[1]

[1]Laboratory of Plasma Electronics, Tomsk State University of Control Systems and Radioelectronics, Tomsk 634050, Russia and [2]Laboratory of Plasma Sources, High Current Electronics Institute, Tomsk 634055, Russia

Research Article

Cite this article: Klimov A, Bakeev I, Oks E, Zenin A (2019). Forevacuum plasma source of continuous electron beam. *Laser and Particle Beams* **37**, 203–208. https://doi.org/10.1017/S0263034619000375

Received: 5 March 2019
Revised: 22 March 2019
Accepted: 1 April 2019

Key words:
Dielectric treatment; electron beam; forevacuum; plasma source

Author for correspondence:
Aleksandr Klimov, Laboratory of Plasma Electronics, Tomsk State University of Control Systems and Radioelectronics, Tomsk 634050, Russia. E-mail: klimov@main.tusur.ru

Abstract

We describe here the design, main parameters, and characteristics of a forevacuum-pressure plasma-cathode electron source based on a hollow-cathode discharge. The source generates a continuous focused electron beam with energy up to 30 keV and current up to 300 mA at a pressure of 10–50 Pa. The focused electron beam reaches a maximum power density of 10^6 W/cm^2. The source utility has been demonstrated by its application for processing and cutting of ceramic.

Introduction

Electron sources with plasma cathodes are a type of electron-beam device that operates based on electron emission from the plasma of a glow or arc discharge (Oks, 1992; Devyatkov *et al.*, 2015; Koval *et al.*, 2015). The main advantage of the plasma electron sources is its ability to operate at a higher pressure compared with hot-cathode sources (Gleizer *et al.*, 2003; Burdovitsin and Oks, 2008). Plasma electron sources are not demanding with respect to gas atmosphere and vacuum conditions, have a long life, and high emission current density. High temperature of the electrons in the beam, as compared with hot-cathode sources, does not allow using such sources to generate beams of high brightness typical of hot-cathode sources. However, recent studies indicate that this difference is not so great (Kornilov *et al.*, 2009; Bakeev *et al.*, 2018*a*, 2018*b*). As of today, there have been a large number of plasma electron sources being developed varying in design, parameters, and applications (Gleizer *et al.*, 2003; Burdovitsin and Oks, 2008; Kornilov *et al.*, 2009; Devyatkov *et al.*, 2015; Akishev *et al.*, 2017; Akishev *et al.*, 2018; Bakeev *et al.*, 2018*a*, 2018*b*). Among the most needed applications of plasma electron sources, one can highlight welding, metal and alloy melting, dimensional processing, evaporation and subsequent surface coating, medical instrument treatment, and even food sterilization (Kim *et al.*, 2015; Węglowski *et al.*, 2016; Pillai and Shayanfar, 2017).

The so-called forevacuum-pressure plasma sources, which enable processing of nonconductive dielectric materials (ceramics, polymers, glasses, etc.), occupy a special place in the total assortment of plasma electron sources (Goreev *et al.*, 2012; Burdovitsin *et al.*, 2013; Bakeev *et al.*, 2018*a*, 2018*b*). These sources operate in a pressure range from a few to a few tens of pascals, which is one or two orders of magnitude higher than the working pressure of conventional plasma sources (Zenin *et al.*, 2013). At such pressure, the electron beam transport is accompanied by the formation of plasma with a concentration of order 10^{16}/m^3, which is sufficient to practically compensate the negative charge carried by the beam electrons onto the irradiated target (Burdovitsin *et al.*, 2009). The electric potential of the target surface within the processed area does not exceed several hundreds of volts and does not noticeably change the electron beam energy, much less deflect it off the processed area as is the case at higher vacuum. Thus, in the forevacuum range of pressure, the energy transfer to the irradiated target is close to 100%, which is an undoubted advantage of such type of sources.

Here we present the design, main parameters, and characteristics of the latest modifications of the forevacuum plasma electron source based on a hollow-cathode discharge which provides higher values of the electron beam-specific parameters.

Forevacuum plasma electron source

An illustration and a photograph of the forevacuum plasma electron source are shown in Figure 1.

The design of the electron source consists of two main units: a discharge cell to generate the emission plasma, and the electron extraction and acceleration system. The plasma electron sources normally use a glow or an arc discharge to generate plasma (Oks, 2006). The most suitable discharge system for generation of the emission plasma in the forevacuum pressure range is a hollow-cathode glow discharge, wherein electron selection is carried out through an anode emission aperture (Oks, 2006). This kind of discharge is preferable because of its broad range of working pressure, fully corresponding to the forevacuum pressure range, the

© Cambridge University Press 2019

CAMBRIDGE UNIVERSITY PRESS

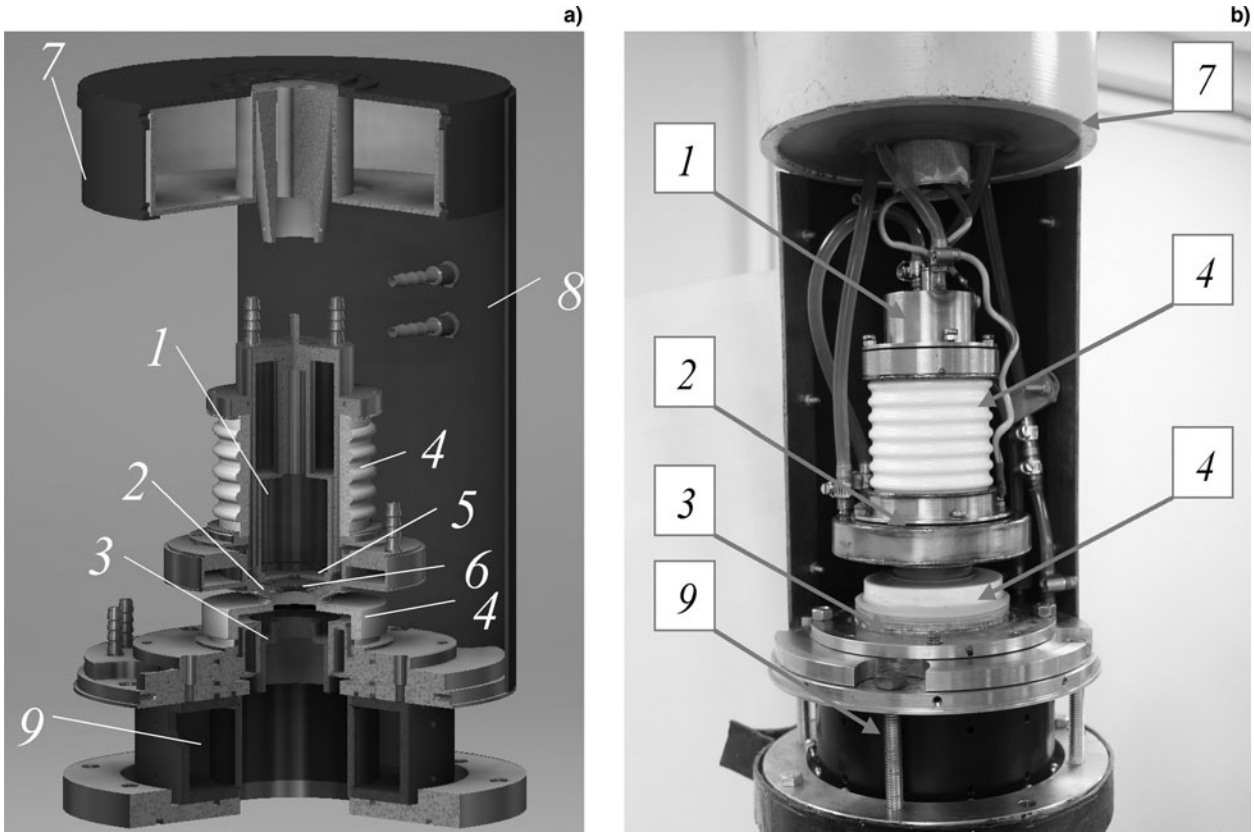


Fig. 1. Illustration (a) and (b) photograph of the forevacuum plasma electron source. 1 – hollow cathode; 2 – plane anode; 3 – extractor; 4 – metal-ceramic insulator; 5 – cathode replacement insert; 6 – tantalum emission electrode; 7 – caprolon cylinder with water high-voltage isolator; 8 – steel body frame; 9 – body of the magnetic lens.

possibility to create a high-density plasma in a small volume, relatively low discharge burning voltage, temporal stability of parameters, as well as the possibility to shape the extracted electron beam by changing the geometry of the plasma emission boundary (White, 1959; Sturges and Oskam, 1964; Burdovitsin and Oks, 1999).

The forevacuum plasma electron source is basically a three-electrode system: hollow cathode 1, plane anode 2, and extractor 3. The source electrodes are electrically insulated using standard metal-ceramic insulators 4. These insulators also serve as a bearing structure for the source. The hollow cathode and the plane anode make up the electron source discharge system. The hollow cathode is a cylinder with an outer radius of 55 mm; the inner part of the cathode cavity is 110 mm deep and consists of two sections of different diameters d_1 and d_2, and lengths l_1 and l_2; see Figure 1. The length of the section's narrow part, located in the region of the cavity opposite to the anode, can vary from 10 to 90 mm. The diameter of the narrow part varies from 8 to 40 mm. The diameter of the wider part is 40 mm. The cathode walls are enclosed in a cooling water jacket. In the wider part of the hollow cathode, there is a threaded hole for screwing replacement insert 5. The insert has an 8 mm-diameter hole and due to varying anode–cathode separation makes it possible to change the emission conditions and the area of the open plasma boundary from which the electrons can reach the anode, thus allowing control of the magnitude of the extracted current to some extent. The anode is shaped as a disk with a 15 mm-diameter hole in the center and has a cooling water jacket. The anode

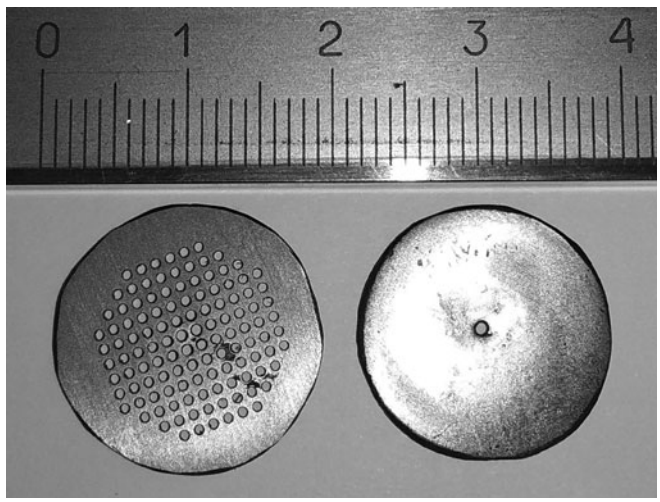


Fig. 2. Photograph of multi-aperture and single-aperture emission electrodes.

aperture is closed by a 1 mm-thick tantalum plate (emission electrode) 6. This plate has either one emission aperture of 1.5 mm diameter or multiple 0.7 mm apertures (Fig. 2). The anode area from which the emission occurs (a circle of about 10 mm diameter) allows no more than 120 holes of 0.7 mm diameter. The diameter values of 1.5 mm and 0.7 mm for the emission aperture were chosen in order to provide a stable and effective operation of the plasma electron source. At a diameter >1.5 mm, the plasma boundary shifts

https://doi.org/10.1017/S0263034619000375 Published online by Cambridge University Press

to the accelerating gap, provoking a diminished dielectric strength of the gap. At a diameter <0.7 mm, the efficiency of electron emission from the plasma decreases significantly. Electron emission from a single aperture provides high electron beam power density, while emission from the multiple-aperture electrode yields high electron beam total current and power. Plate 6 fixes the plasma boundary and plays the same stabilizing role as the emission grid (Oks, 2006). Extractor 3 is made of stainless steel and shaped as a truncated cone, with a 15 mm-diameter aperture to allow for the beam passage, threaded on the outer cylindrical surface to make it possible to move it along the system axis. The extractor, as usual, is grounded and the negative pole of the high-voltage source is connected to the anode.

The anode and cathode are cooled by running water. The water pumping rate through the cooling system maintains the electrode at a temperature not exceeding 30°C. Since the cooled electrodes (anode and cathode) are at a high electric potential with respect to ground, the electron source design provides for installation of a high-voltage insulating water cooling section. The water high-voltage isolator is designed as a plastic tube with an inner diameter 6 mm and a length 4 m. The tube is spiraled onto caprolon cylinder 7. The spiral coils are padded with additional insulating layers. The electron source and the water-cooling system are encased in a 2 mm-thick steel body 8, which effectively protects from X-ray bremsstrahlung radiation. The source electrodes are accessed through a detachable body segment.

The plasma electron source is fed by direct voltage power supply units E1 and E2 connected, respectively, to the discharge and the accelerating gaps. The discharge current I_d varies from 0.1 to 1.5 A at a discharge burning voltage of 300–700 V. In the gap between anode 2 and extractor 3, upon applying a corresponding voltage, electron acceleration and initial beam formation take place. The accelerating voltage U_a during emission from the single aperture varies from 0.5 to 30 kV and is limited by the onset of intensive X-ray bremsstrahlung radiation. During emission from the multiple-aperture electrode, the accelerating voltage U_a, due to the electrode thermal deformation, is limited to a value of 20 kV. The electron beam formed by the source is focused by magnetic lens 9 which also serves as a structural unit of the electron source. The beam current I_b varies within the range of 10–350 mA independently of the accelerating voltage. The beam current I_b is measured with the help of a Faraday cup.

The source operates under an isobaric gas regime because at forevacuum pressure conditions one would fail to create a pressure drop between the plasma generation and the beam formation regions. The vacuum chamber is pumped down to a pressure of 3 Pa, followed by puffing of the working gas to the required pressure. When changing the working gas, the chamber was first flushed by the new gas for 10–15 min. The pressure was measured by a PfeifferCMR 362 active capacitance gauge whose working principle is independent of the type of gas. A model and a photograph of the electron source are shown in Figure 1. The detachable section of the body is not shown.

Measurements of the electron beam were done using the slit-probe method (Kaur *et al.*, 2015). The essence of the method is based on a continuous and rapid crossing by the beam of two parallel slits behind which is placed a current collector. The collector signal was read by a Tektronix 2024B oscilloscope. The slit width was 100 μm and was selected so as to minimize the measurement error of beam diameter. Because of the small width of the slits, the plasma that is inevitably generated in the forevacuum pressure range along the electron beam propagation path (the "beam-plasma") cannot penetrate the plate with the measuring slits and reach the collector. As a result, the read current signal completely reflects the distribution of beam current density. The slits were separated by 5 mm. A magnetic coil was used to deflect the electron beam. By changing the coil current, it was possible to deflect the beam at a speed up to 100 cm/s.

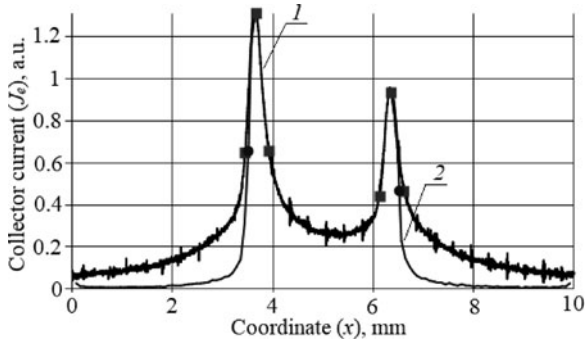


Fig. 3. The oscilloscope probe signal (1) and the calculated beam current density distribution based on it (2).

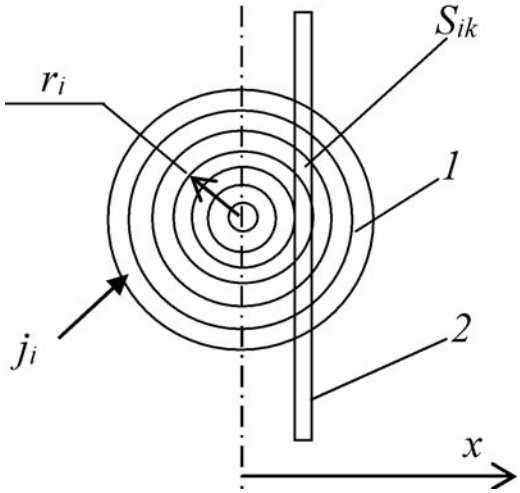


Fig. 4. Calculation of the radial distribution of beam current density: 1 – beam cross section, 2 – measuring slit.

A typical collector current signal read by the oscilloscope is shown in Figure 3 (line 1). Because the beam diameter was calculated based on the radial distribution of beam current density, conversion of the obtained probe distribution $j(x)$ to a radial distribution of beam current density was performed as follows. The distance between the two peaks sets a scale to plot the dependence of probe current density on the coordinate, zero-based at beam center. The coordinate x is calculated as $x = L \cdot t/T$, where L is the separation between the slits, t is time, and T is the oscilloscope time between the maximums. The current density profile is recovered according to the diagram shown in Figure 4.

The electron beam was modeled as a set of tubes with equal current densities $j(r)$. The beam crosscut is made up of a set of concentric rings i enumerated beginning from the outmost ring. In this case, the current density profile is

$$j_e(x_i) = \frac{J_e(x_i) - 2d\sum_{k=2}^{i} j_e(x_{n-1})\left(\sqrt{x_{n-1}^2 - x_i^2} - \sqrt{x_n^2 - x_i^2}\right)}{2d\sqrt{x_i^2 - x_{i+1}^2}},$$

https://doi.org/10.1017/S0263034619000375 Published online by Cambridge University Press

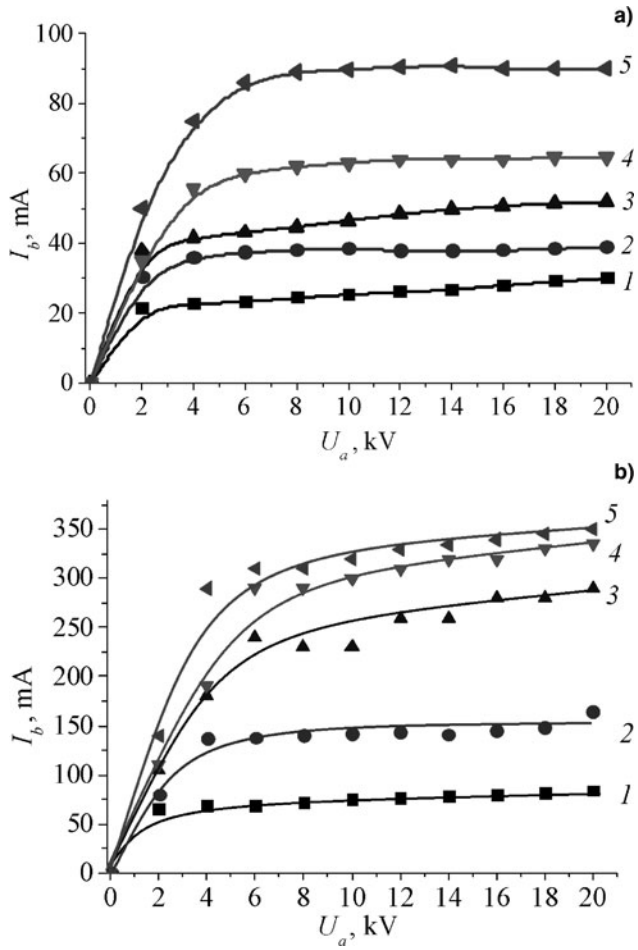


Fig. 5. Dependence of beam current on the accelerating voltage for different emission electrodes: (a) single-aperture, (b) multiple-aperture emission electrode. Discharge current: (1) 300 mA, (2) 600 mA, (3) 900 mA, (4) 1200 mA, (5) 1500 mA.

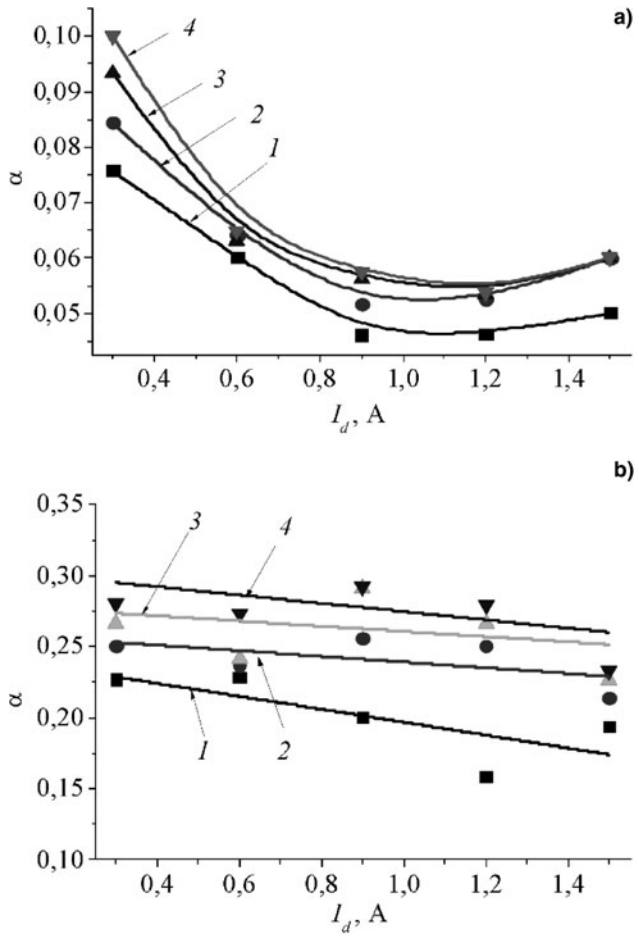


Fig. 6. Dependences of the electron extraction efficiency on discharge current for the two types of emission electrodes: (a) single-aperture, (b) multiple-aperture emission electrodes. Accelerating voltage: (1) 5 kV, (2) 10 kV, (3) 15 kV, (4) 20 kV.

where $J_e(x_i)$ is the current measured at the collector at the point x_i, and $j_e(x_i)$ is the recovered radial profile of the current density at the cross-section at x_i.

A typical radial distribution of beam current density $j(r)$ calculated based on the probe signal is shown in Figure 3 (line 2). The beam diameter d_b is assumed equal to the width at the half height of the recovered current density distribution.

Parameters and characteristics of the electron source

The source voltage–current characteristic for the single-aperture and the multiple-aperture emission electrodes is shown in Figure 5. As seen in Figure 5, the source voltage–current characteristic contains two regions with a close to linear dependence which have different slopes relative to the horizontal axis. Within the range of accelerating voltage 2–4 kV (depending on the discharge current), a sharp increase in the collector current is observed which then slows down and a saturation trend appears, demonstrating behavior characteristic of plasma electron sources and confirming the presence of an accelerated electron beam.

The electron extraction efficiency $\alpha = I_b/I_d$ (ratio of the beam current to the discharge current) is an important parameter describing the electron source. The dependences of electron extraction efficiency on the discharge current for the two types of emission electrodes are shown in Figure 6.

As should be expected, the most efficient electron extraction is observed for emission using multiple apertures. The efficiency of electron extraction through the multiple-aperture electrode reaches 0.32, while the maximum efficiency for the single-aperture emission does not exceed 0.1. Besides, an increase of the discharge current lowers the extraction efficiency from the single aperture by a factor of two, which is apparently due to current interception by the anode. In the case of the emission from multiple apertures, the drop-off of efficiency is observed only at small values of the accelerating voltage, <5 kV. With an increase of the accelerating voltage, the efficiency increases and remains practically constant for the whole range of discharge current.

Since electron sources are designated for electron-beam processing of dielectric materials, including those with an intense gas release during irradiation (e.g., ceramic or metal powders), the gas pressure in the working chamber during electron-beam treatment can increase by a factor of several. In this regard, we have studied the dependence of the electron beam diameter on the vacuum chamber pressure.

The dependence of beam diameter on pressure for the single-aperture emission is shown in Figure 7 and for the multiple-aperture electrode in Figure 8.

https://doi.org/10.1017/S0263034619000375 Published online by Cambridge University Press

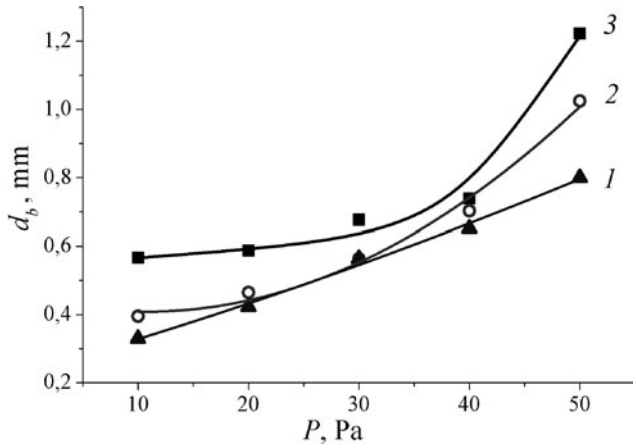


Fig. 7. Dependence of the beam diameter on pressure for the single-aperture emission at different beam current: (1) 15 mA, (2) 30 mA, (3) 90 mA. The accelerating voltage is 30 kV.

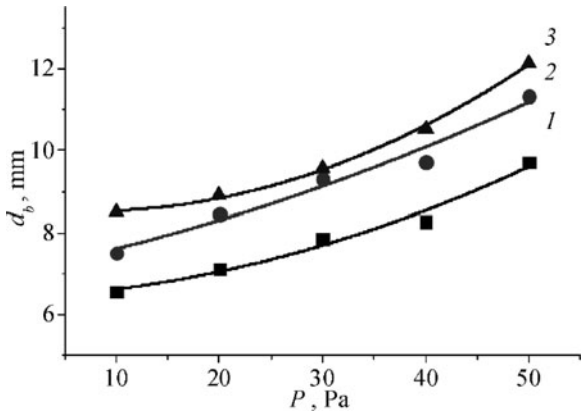


Fig. 8. Dependence of the beam diameter on pressure for the emission from multiple apertures at different beam current: (1) 50 mA, (2) 100 mA, (3) 150 mA. The accelerating voltage is 20 kV.

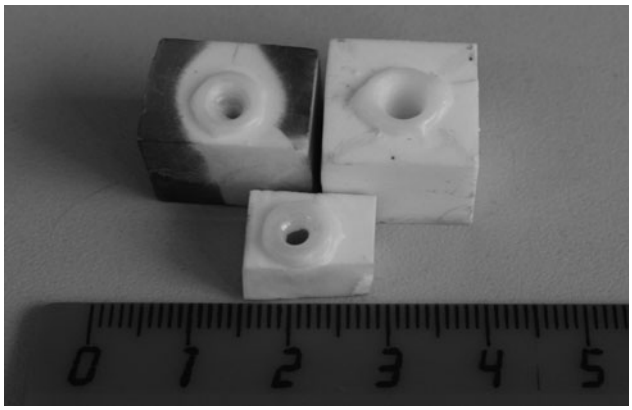


Fig. 9. Samples of alumina ceramic with a hole made by the electron beam.

The dependences of the electron beam diameter for different numbers of apertures determine the possible applications of the forevacuum plasma electron source we have described. For the single aperture, one can create a narrow beam with diameter <0.8 mm over a broad range of helium pressure, 10–40 Pa, and an electron beam power density of 10^6 W/cm^2. In the case of the multiple-aperture emission electrode, the beam power density of 10^4 W/cm^2 is two orders of magnitude less. Thus, the electron beam emitted from the single aperture can be used for localized action on dielectrics (ceramics, polymers, glass, etc.). The emission from the multiple-aperture electrode makes it attractive to use such electron beams for material heating and melting.

The use of a low-power density beam with a diameter of several millimeters allows heating large areas of alumina ceramics and weld tubes with a diameter up to 20 mm. The emission from the single aperture can be applied for milling and drilling deep holes in ceramic or glass, of diameter <1 mm and up to 70 mm deep (Fig. 9).

Conclusion

In this paper, we have presented the design and main parameters of a plasma electron source capable of generating an electron beam over a wide range of pressure, 10–50 Pa. We have explored the primary characteristics of the electron beam (beam current, beam diameter, power density) depending on the electron source parameters for two types of emission electrodes.

It is shown that, depending on the number of apertures made in the emission electrode, there are realized different beam generation regimes: in the case of a single aperture, the generated beam has a power density of 10^6 W/cm^2 and a diameter of 0.8 mm and is suitable for performing localized action on materials; in the case of 120 apertures, the beam diameter is 6–12 mm and the power is 3 kW making such beams attractive in applications requiring heating, melting, and evaporation of materials.

Author ORCIDs. Ilya Bakeev, 0000-0001-6807-3757.

Acknowledgements. This work was supported in part by the Russian Foundation for Basic Research, grant No 18-38-20007. E.O. is the executor of work on the topic "Organization of scientific research" No. 3.6441.2017/6.7. Special thanks to Dr. Ian Brown (Berkeley Lab) for English correction and useful discussion.

References

Akishev YS, Karalnik VB, Medvedev MA, Petryakov AV, Trushkin NI and Shafikov AG (2017) 25 keV electron beam formation based on a three-electrode system of the obstructed glow discharge in H2 and D2. *Journal of Physics: Conference Series* **830**, 012015.

Akishev Y, Aponin G, Karalnik V, Petryakov A and Trushkin N (2018) Three-electrode strongly overvoltage open discharge in D 2 as an effective source of the high-current beam of runaway electrons with energy up to 25 keV. *Journal of Physics D: Applied Physics* **51**, 394003.

Bakeev IY, Dvilis ES, Klimov AS, Oks EM and Zenin AA (2018*a*) The possibilities of dimensional electron-beam processing as applied to selective sintering of oxide ceramics in the forevacuum pressure range. *Journal of Physics: Conference Series* **945**, 012016.

Bakeev IY, Klimov AS, Oks EM and Zenin AA (2018*b*) Generation of high-power-density electron beams by a forevacuum-pressure plasma cathode electron source. *Plasma Sources Science and Technology* **27**, 075002.

Burdovitsin V and Oks E (1999) Hollow-cathode plasma electron gun for beam generation at forepump gas pressure. *Review of Scientific Instruments* **70**, 2975–2978.

Burdovitsin VA and Oks EM (2008) Fore-vacuum plasma cathode electron sources. *Laser and Particle Beams* **26**, 619–635.

Burdovitsin VA, Klimov AS and Oks EM (2009) On the possibility of electron-beam processing of dielectrics using a forevacuum plasma electron source. *Technical Physics Letters* **35**, 511–513.

https://doi.org/10.1017/S0263034619000375 Published online by Cambridge University Press

Burdovitsin V, Dvilis ES, Zenin A, Klimov A, Oks E, Sokolov V, Kachaev A and Khasanov OL (2013) Electron beam sintering of zirconia ceramics. *Advanced Materials Research* **872**, 150–156.

Devyatkov VN, Vorobyov MS, Koval NN and Shugurov VV (2015) Modernization of cathode assemblies of electron sources based on low pressure arc discharge. *Journal of Physics: Conference Series* **652**, 012066.

Gleizer JZ, Krokhmal A, Krasik YE and Felsteiner J (2003) Generation of high-current electron beams by a hollow cathode with a ferroelectric plasma source. *The European Physical Journal D – Atomic, Molecular and Optical Physics* **26**, 285–295.

Goreev AK, Burdovitsin VA, Klimov AS and Oks EM (2012) Electron beam welding of ceramic to metal using fore-vacuum plasma electron source. *Inorganic Materials: Applied Research* **3**, 446–449.

Kaur A, Ribton C and Balachandaran W (2015) Electron beam characterization methods and devices for welding equipment. *Journal of Materials Processing Technology* **221**, 225–232.

Kim SM, Fan H, Cho YJ, Eo MY, Park JH, Kim BN, Lee BC and Lee SK (2015) Electron beam effect on biomaterials I: focusing on bone graft materials. *Biomaterials Research* **19**, 10.

Kornilov SY, Osipov IV and Rempe NG (2009) Generation of narrow focused beams in a plasma-cathode electron gun. *Instruments and Experimental Techniques* **52**, 406–411.

Koval TV, Devyatkov VN, Nguyen BH and Uglov VV (2015) Plasma-cathode electron source based on a low-pressure arc discharge in the mode of the emission current enhancement. *High Temperature Material Processes* **19**, 19–27.

Oks EM (1992) Physics and technique of plasma electron sources. *Plasma Sources Science and Technology* **1**, 249–255.

Oks EM (2006) *Plasma Cathode Electron Sources – Physics, Technology, Applications*. New York: Wiley-VCH.

Pillai SD and Shayanfar S (2017) Electron beam technology and other irradiation technology applications in the food industry. In Venturi M and D'Angelantonio M (eds), *Applications of Radiation Chemistry in the Fields of Industry, Biotechnology and Environment*. Cham: Springer, pp. 249–268.

Sturges DJ and Oskam HJ (1964) Studies of the properties of the hollow cathode glow discharge in helium and neon. *Journal of Applied Physics* **35**, 2887–2894.

Węglowski MS, Błacha S and Phillips A (2016) Electron beam welding – techniques and trends – review. *Vacuum* **130**, 72–92.

White AD (1959) New hollow cathode glow discharge. *Journal of Applied Physics* **30**, 711–719.

Zenin AA, Klimov AS, Burdovitsin VA and Oks EM (2013) Generating stationary electron beams by a forevacuum plasma source at pressures up to 100 Pa. *Technical Physics Letters* **39**, 454–456.

https://doi.org/10.1017/S0263034619000375 Published online by Cambridge University Press